



The chemical ecology of coumarins and phenazines affects iron acquisition by pseudomonads

Darcy L. McRose^{a,b,1,2}, Jinyang Li^a, and Dianne K. Newman^{a,b,2}

Edited by Mary Lou Guerinot, Dartmouth College, Hanover, NH; received October 27, 2022; accepted February 27, 2023

Secondary metabolites are important facilitators of plant–microbe interactions in the rhizosphere, contributing to communication, competition, and nutrient acquisition. However, at first glance, the rhizosphere seems full of metabolites with overlapping functions, and we have a limited understanding of basic principles governing metabolite use. Increasing access to the essential nutrient iron is one important, but seemingly redundant role performed by both plant and microbial Redox-Active Metabolites (RAMs). We used coumarins, RAMs made by the model plant *Arabidopsis thaliana*, and phenazines, RAMs made by soil-dwelling pseudomonads, to ask whether plant and microbial RAMs might each have distinct functions under different environmental conditions. We show that variations in oxygen and pH lead to predictable differences in the capacity of coumarins vs phenazines to increase the growth of iron-limited pseudomonads and that these effects depend on whether pseudomonads are grown on glucose, succinate, or pyruvate: carbon sources commonly found in root exudates. Our results are explained by the chemical reactivities of these metabolites and the redox state of phenazines as altered by microbial metabolism. This work shows that variations in the chemical microenvironment can profoundly affect secondary metabolite function and suggests plants may tune the utility of microbial secondary metabolites by altering the carbon released in root exudates. Together, these findings suggest that RAM diversity may be less overwhelming when viewed through a chemical ecological lens: Distinct molecules can be expected to be more or less important to certain ecosystem functions, such as iron acquisition, depending on the local chemical microenvironments in which they reside.

phenazine | coumarin | pseudomonas | redox | secondary metabolite

Secondary metabolites are increasingly appreciated for their role in regulating plant–microbe and microbe–microbe interactions in the rhizosphere (1–4). Yet, the rhizosphere is home to numerous plant and microbial metabolites with seemingly chemically redundant properties. This presents a paradox: If these molecules are in fact redundant, why are there so many of them? One potential answer is that our ability to assess their functional redundancy has been limited by an imperfect understanding of the different chemical niches they occupy. Considering the steep chemical gradients that characterize most microbial systems (5–8), it is tempting to speculate that dynamic chemical changes in time and space might impose constraints upon the reactivity of secondary metabolites, conferring more nuanced functions and greater specificity to these molecules. In other words, a chemical ecological framework might help explain this apparent paradox.

Testing this idea demands specificity, thus we focused on the essential metal iron (Fe) and its role in soil ecosystems. Increasing access to iron is one important, completely understood role for soil secondary metabolites. In oxygenated environments, iron often precipitates as Fe(III)-oxyhydroxides, which can be relatively unavailable. Plants and microbes have developed several strategies to increase iron bioavailability: The production of Fe(III)-binding molecules such as siderophores or phytosiderophores, the reduction of Fe(III) to Fe(II) by Redox-Active Metabolites (RAMs), and rhizosphere acidification (9). Siderophore and RAM production is widespread in bacteria, with many organisms producing both types of metabolites. Secondary metabolite production is more divided in plants—true grasses tend to make phytosiderophores, while RAM production is used by all other plants (9).

It has long been recognized that siderophores, which form complexes with iron that can only be accessed via specialized molecular machinery, might facilitate microbial competition by regulating access to iron (10–14). Recent work with synthetic microbial communities has shown that the presence of different siderophore producers can shape rhizosphere microbial communities, contributing to both the suppression and proliferation of plant pathogens (2, 15). We know far less about the role of RAMs than siderophores in regulating iron availability in soil microbial communities, and most studies (on both

Significance

Plant–microbe interactions in the rhizosphere affect plant growth, carbon storage, and agriculture and are frequently governed by small molecules called secondary metabolites. We tested the idea that plant coumarins and bacterial phenazines, redox-active secondary metabolites capable of performing the same function (iron solubilization) might have distinct chemical niches. We found that coumarins solubilized iron and stimulated microbial growth under high and low oxygen and pH. Phenazines were restricted to low oxygen and pH but growth on glucose alleviated this restriction by allowing microbes to shift the phenazine redox state. Because root exudates are a major source of rhizosphere carbon, our results also suggest that plants may indirectly influence bacterial metabolite reactivity by altering carbon release.

Author contributions: D.L.M. and D.K.N. designed research; D.L.M. and J.L. performed research; D.L.M., J.L. and D.K.N. analyzed data; and D.L.M. and D.K.N. wrote the paper.

The authors declare no competing interest.

This article is a PNAS Direct Submission.

Copyright © 2023 the Author(s). Published by PNAS. This article is distributed under Creative Commons Attribution-NonCommercial-NoDerivatives License 4.0 (CC BY-NC-ND).

¹Present address: Department of Civil and Environmental Engineering, Massachusetts Institute of Technology, Cambridge, MA 02139.

²To whom correspondence may be addressed. Email: dmcrose@mit.edu or dkn@caltech.edu.

This article contains supporting information online at <https://www.pnas.org/lookup/suppl/doi:10.1073/pnas.2217951120/-/DCSupplemental>.

Published March 30, 2023.

RAMs and siderophores) have focused on either plant or microbial metabolites rather than interactions between the two. Yet, much evidence points to RAMs as important players in soil iron cycling and the chemical properties of RAMs make them particularly sensitive to changes in chemical conditions, suggesting that different RAMs may be more or less useful in different environmental contexts.

As a test case, we focused on plant coumarins and bacterial phenazines, well-studied model RAMs that are likely to co-occur in the rhizosphere. Coumarins are made by numerous plants including the model plant *Arabidopsis thaliana* (16) and are crucial for plant growth under iron limitation (17–20). Studies exploring the effects of coumarins on rhizosphere bacteria have focused on their toxicity (mostly through the generation of reactive oxygen species, ROS) and capacity to suppress specific members of the root microbiome (3, 4, 16). The potential growth benefits of coumarins for iron-limited soil bacteria and any interactions with the endogenous metabolites made by these organisms remain largely unexplored. Phenazines are one such set of bacterially-produced RAMs, which, like coumarins, have antibiotic properties owing to ROS generation, but can also help to solubilize iron (21–23). Phenazines are made by numerous soil-dwelling bacteria (24), and in pseudomonads, some of their best-studied producers, phenazines have been shown to liberate excess quantities of iron needed to promote biofilm formation (25).

Despite their seeming similarities, differences in the reactivities of coumarins and phenazines hint that these metabolites may be useful for iron solubilization under different conditions (Fig. 1). RAMs liberate iron through electron transfer from the metabolite to Fe(III), which means that RAMs are only able to solubilize iron in their reduced, electron carrying state. Reduced phenazines are highly reactive with oxygen, often reducing O_2 to O_2^- (21), a process that oxidizes the phenazine. Reduced coumarins, in contrast, appear to be less reactive with oxygen (26, 27). In addition, phenazines are (re)reduced by pseudomonads; reducing power, in the form of a carbon source, is essential for this process (28, 29). The importance of carbon source for phenazine reduction is especially intriguing in the rhizosphere where plant root exudates are a key source of carbon, raising the possibility that changes in these exudates may alter secondary metabolite utility.

We hypothesized that variations in oxygen, pH and carbon source might shift RAM redox state, creating distinct chemical niches for coumarins as opposed to phenazines. Our work centers on the specific case of RAM solubilization of iron, but our primary goal was to explore the broader idea that secondary metabolites might be better understood through consideration of their local chemical context. We tested this idea through chemical characterizations of coumarins and phenazines as well as growth experiments with pseudomonads cultured under different oxygen tensions, across varying pH, and on succinate, glucose, and pyruvate—carbon sources found in root exudates (30–32). Our results shed light on the chemical ecology of iron solubilization by RAMs in the rhizosphere and suggest a previously unappreciated mechanism by which root exudates may tune the utility of microbial secondary metabolites.

Results and Discussion

Structurally Diverse Coumarins Have Different Redox Potentials and Reactivities with Iron and Oxygen. Both coumarins and phenazines can reduce Fe(III) (19, 21, 33). As a basis for identifying the different chemical niches that they might occupy, we used cyclic voltammetry (CV), a standard electrochemical method for the characterization of redox-active metabolites (34). Many studies have probed the electrochemical properties of various coumarins and phenazines; however, few have compared voltammograms across metabolites and pH. In order to capture a range of coumarin structures we tested: coumarin, 7,8-dihydroxycoumarin (daphnetin), 7,8-dihydroxy-6-methoxycoumarin (fraxetin), and 7-hydroxy-6-methoxycoumarin (scopoletin). Coumarin forms the base scaffold for the other molecules. It was the first to be discovered and was isolated from *Coumarouma odorata*, providing the namesake for the group of molecules (35). Fraxetin and scopoletin are frequently detected in roots exudates from *A. thaliana*, with scopoletin being especially abundant (4, 17). Daphnetin is produced by members of the *Daphne* species. We focused on phenazine-1-carboxylic acid (PCA) because this is the phenazine most commonly made by soil-dwelling pseudomonads and has been detected in plant rhizospheres (36). Daphnetin and fraxetin showed clear oxidation and reduction peaks (Fig. 2A),

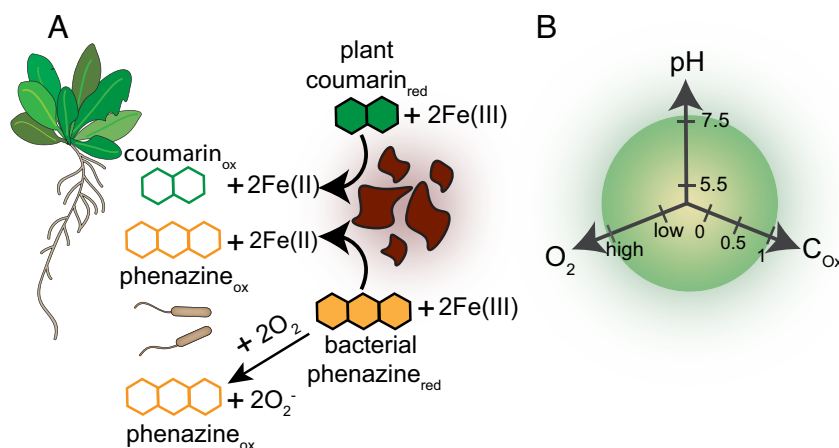


Fig. 1. The chemical ecology of rhizosphere redox-active metabolites (RAMs) may help resolve their seemingly redundant functions. (A) Plant coumarins (green) and bacterial phenazines (orange) are both RAMs that aid in iron solubilization, yet it is unknown whether changes in environmental chemistry may favor one type of metabolite over another. One notable difference between the metabolites is that phenazines are more reactive with oxygen than coumarins. (B) We can predict distinct chemical ecological niches where coumarins and phenazines may be more effective at promoting iron acquisition over a regime defined by variable oxygen, pH, and carbon exudate concentrations. Phenazines (orange) may be most useful in environments where they can be easily reduced by microbes: under low pH, low O_2 , and in the presence of reduced carbon sources. Coumarins (green) are not as reactive with oxygen and do not require microbial reduction to liberate iron, potentially making them useful across a wide range of environmental conditions. (C_{ox}): carbon oxidation state.

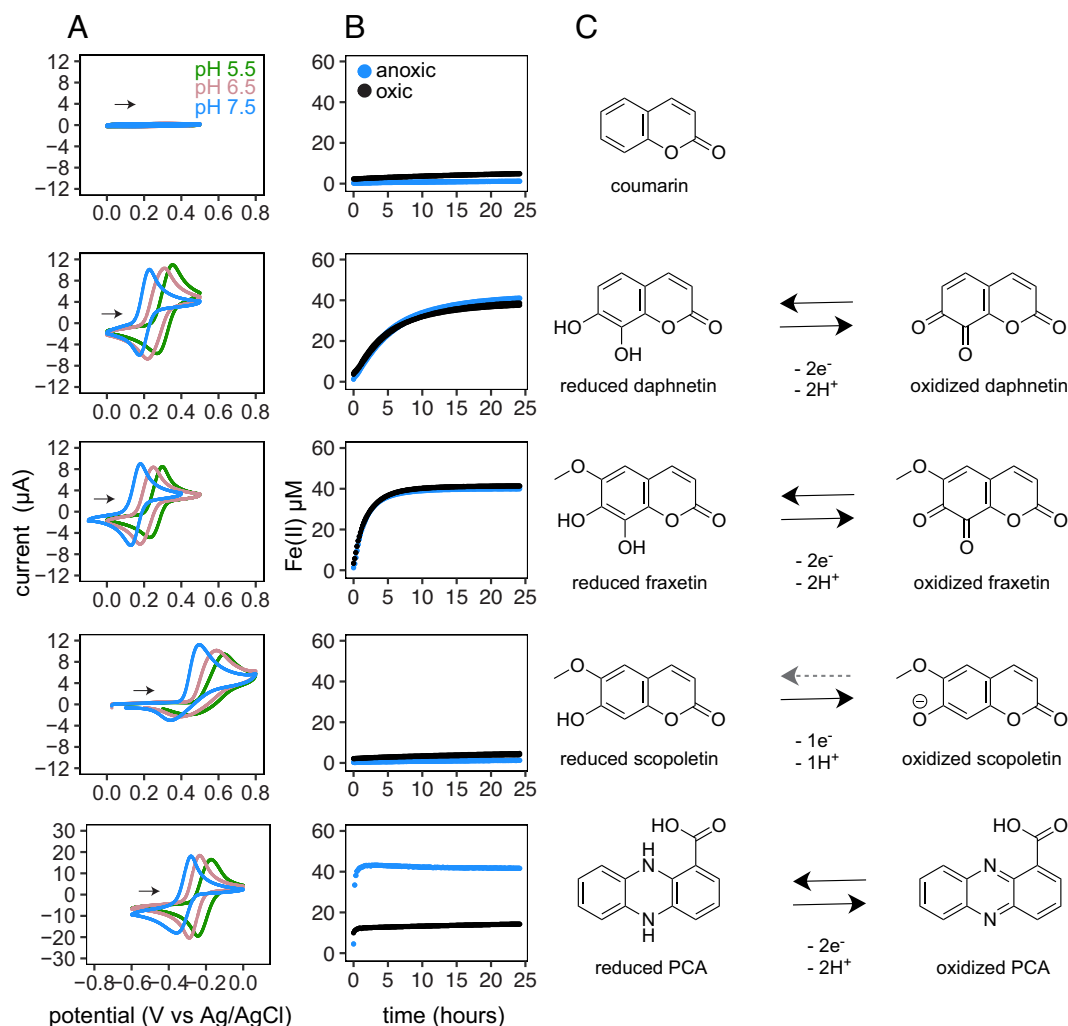


Fig. 2. Chemical properties of coumarins and the phenazine PCA. (A) Voltammograms showing reversible redox activity of daphnetin, fraxetin, and PCA at pH 5.5, 6.5, and 7.5. Experiments were conducted with 1 mM metabolite under ambient oxygen (coumarins) or N₂ (PCA). The CV profile of scopoletin is complex (37), see *SI Appendix, Fig. S1*. Coumarin CV experiments used a gold working electrode, PCA CV used a glassy carbon working electrode (*Materials and Methods*). Note large scale difference in potentials between coumarins and PCA. (B) Iron reduction by different metabolites in the presence (black) or absence (blue) of oxygen. Experiments were conducted at pH 7.5 with 40 μM Fe(III) as FeCl₃ and 20 μM of each metabolite, Fe(II) was detected with the ferrozine assay and shows 2:1 metabolite:Fe(II) stoichiometry. See *SI Appendix, Figs. S2 and S3* for further controls and experiments at pH 5.5. Duplicate assays are shown as two separate lines. (C) Structures of oxidized and reduced coumarins and PCA. Redox reactions involving scopoletin are complex and only one potential oxidation product is shown (37). Metabolites used in A and B are indicated in panel C.

consistent with reversible redox reactions, as has been previously reported (19). In contrast, coumarin did not exhibit redox activity and scopoletin showed a complex CV profile with very wide peak separation and much higher oxidative than reductive peak, suggesting an irreversible reaction. Subsequent scans of scopoletin (*SI Appendix, Fig. S1*) showed a decrease in the oxidative peak possibly due to polymerization of oxidation products and interactions at the electrode surface (37). As expected, PCA also showed reversible redox behavior, although voltammograms were slightly more complex at higher pH (*Materials and Methods, (21)*). In addition, the potentials of the oxidative and reductive peaks for daphnetin, fraxetin, scopoletin, and PCA shifted with pH, as expected for proton-coupled redox reactions (Fig. 2 A and C). The different coumarins showed a range of redox potentials, with scopoletin being the most positive followed by daphnetin and then fraxetin. Consistent with previous findings (19, 21), the calculated midpoint redox potentials of all three molecules were more than 400 mV more positive than those for PCA (Fig. 2A and *SI Appendix, Table S1*).

We used the ferrozine assay, a colorimetric assay for Fe(III) reduction, as a means to probe the reactions between Fe(III), O₂,

and RAMs. In order to reduce Fe(III), RAMs must be in their reduced state (Figs. 1A and 2C). If RAMs are oxidized by oxygen before they can react with Fe(III), their Fe(III) reduction capacity should be diminished. We therefore compared Fe(III) reduction in anoxic and oxic conditions. Under anoxic conditions daphnetin, fraxetin, and PCA showed clear iron reduction, whereas coumarin did not, as expected for a metabolite without redox activity (Fig. 2B and *SI Appendix, Fig. S2*). Scopoletin was slightly more complicated, this metabolite did not show Fe(III) reduction at pH 7.5 (Fig. 2B) but did show limited Fe(III) reduction at pH 5.5 (*SI Appendix, Fig. S2*), consistent with the more positive redox potential of this metabolite (*SI Appendix, Table S1*), which is likely too high to reduce Fe(III) at pH 7.5. Despite all exhibiting redox reversibility, daphnetin, fraxetin, and PCA behaved very differently when iron reduction experiments were performed under oxic vs anoxic conditions. While oxygen had very little effect on daphnetin and fraxetin, it stunted iron reduction by PCA: Fe(II) accumulation flattened around 10 μM , reflecting the rapid oxidation of PCA by oxygen (21, 38). Fe(II) can be rapidly oxidized by oxygen, especially at high pH (39) which could also account for diminished accumulations of Fe(II) in PCA

experiments. However, control experiments conducted with Fe(II) alone (*Materials and Methods* and *SI Appendix*, Fig. S3) showed that even under fully oxic conditions, ferrozine rapidly binds Fe(II) before it is oxidized. Hence we attribute the decrease in Fe(II) accumulations in oxic PCA treatments to the oxidation of PCA, not the (re)oxidation of Fe(II). Experiments using air equilibrated PCA (which should be fully oxidized) did not show iron reduction under either oxic or anoxic conditions (*SI Appendix*, Fig. S2). In the absence of oxygen, Fe(III) reduction rates were highly consistent with redox potentials, with PCA which has the most negative redox potential, showing by far the fastest rates followed by fraxetin and daphnetin. These experiments suggest that daphnetin, fraxetin, and PCA are all redox-active metabolites but that daphnetin and fraxetin are not easily oxidized by oxygen whereas PCA is.

Coumarins Capable of Fe(III) Reduction Enhance the Growth of Iron-Limited Pseudomonads. We next asked whether differences in the reactivities of these metabolites translated to their capacity to promote the growth of iron-limited pseudomonads. Due to the variable iron reduction capacity among coumarins (Fig. 2B), we expected that daphnetin and fraxetin, but not coumarin or scopoletin, should be able to enhance growth yields. We also expected that under oxic conditions, PCA would be unable to promote growth. To test this prediction, we induced iron limitation in *Pseudomonas synxantha* and *Pseudomonas aeruginosa* through pregrowth in a defined medium without added iron. Both of these pseudomonads natively produce PCA. *P. synxantha* synthesizes only PCA, whereas *P. aeruginosa* makes PCA in addition to several other phenazines (40). To test the capacity of these metabolites to enhance growth yield when iron is present but relatively unavailable, cultures were supplied with a precipitated iron source (hydrous ferric oxides, HFO) and supplemented with either 100 μ M coumarin, daphnetin, fraxetin, scopoletin, or PCA. For these experiments, both coumarins and PCA were prepared directly from chemical stocks and stored under ambient oxygen conditions without any electrochemical reduction. Oxic conditions were maintained during experiments through constant shaking of culture flasks. Consistent with our expectations, daphnetin and fraxetin enhanced the growth yields of both species while scopoletin provided only modest benefits and coumarin had no effect (Fig. 3 A and B). Notably, very high concentrations of scopoletin in the growth medium of iron-limited *A. thaliana* have been observed (4, 17); hence in natural contexts, this metabolite may contribute to iron solubilization simply due to its high concentrations. As expected, PCA was also unable to rescue growth yields under oxic conditions. Small volume (200 μ L) plate reader experiments at pH 5.5, 6.5, and 7.5 showed similar trends (*SI Appendix*, Fig. S4). Here overall growth yields increased as pH decreased, as would be expected due to increased iron availability at low pH (*SI Appendix*, Fig. S4).

Under iron limitation, pseudomonads make the strong peptidic siderophore pyoverdine as well as the much weaker siderophore pyochelin (41, 42), molecules that might have complex interactions with coumarins. To control for this, we performed experiments using strains of *P. aeruginosa* that have mutations in key siderophore biosynthetic genes (25). Results from these experiments were similar to those from experiments with wild-type *P. aeruginosa*, suggesting that pseudomonads are able to access coumarin-solubilized iron without the aid of siderophores (*SI Appendix*, Fig. S5).

To ensure that growth yield effects were due to increases in the iron supply, we repeated our wild type experiments in a growth medium where nitrogen was limiting but iron was supplied in a

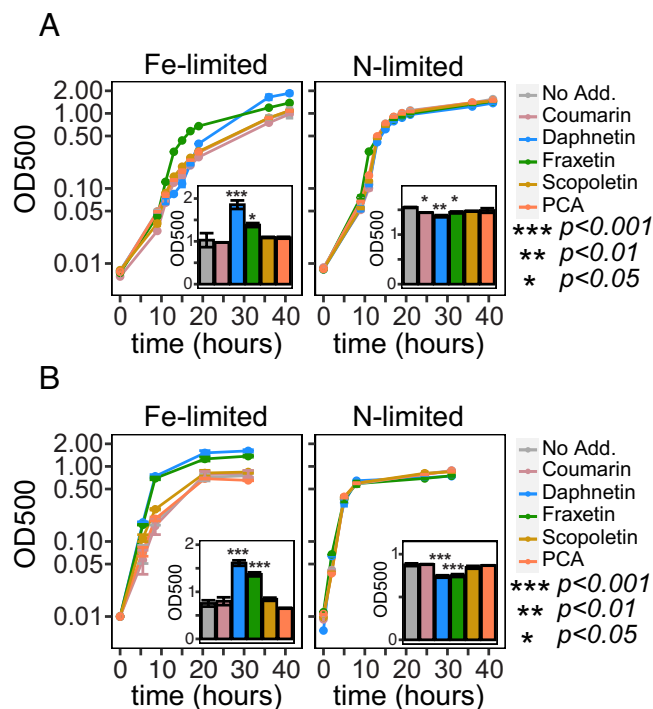


Fig. 3. The coumarins daphnetin and fraxetin stimulate growth of iron-limited pseudomonads. Effect of coumarins and the phenazine PCA on growth of *P. synxantha* (A) and *P. aeruginosa* (B). Under iron-limitation growth yields of both species were enhanced in the presence of daphnetin and fraxetin but not scopoletin, coumarin or PCA (A and B). Under nitrogen limitation, coumarin additions had mildly toxic effects on growth yields (A and B). All experiments used succinate as the carbon source and were conducted at pH 7.5 under ambient oxygen with fully air-equilibrated metabolites, which in the case of PCA leads to metabolite oxidation. The growth medium for Fe-limited experiments used hydrous ferric oxide (HFO) as an insoluble iron source and contained 16 mM N. The growth medium for nitrogen-limited experiments used 100 μ M EDTA and 10 μ M Fe as a soluble iron source and contained 2 mM N. Data shown are for biological duplicates \pm SD. Some error bars may not be visible if they are smaller than the symbol. See also *SI Appendix*, Fig. S4 for additional Fe-limited experiments. Statistical analyses (one-way ANOVA, with Tukey post hoc correction) were performed on data from the final timepoint (*Inset*) and denote significant differences between the indicated treatment and the no addition treatment.

soluble form (10 μ M Fe, 100 μ M EDTA) ethylenediaminetetraacetic acid. Under these conditions, none of the added metabolites increased the final growth yield (Fig. 3). Instead, in this context, daphnetin and fraxetin showed mildly toxic effects leading to small but significant decreases in growth yield (Fig. 3). The mechanisms of iron solubilization by coumarins are complex and incompletely understood—In addition to the capacity to reduce iron, both fraxetin and daphnetin have iron-binding moieties that may allow them to further solubilize and stabilize iron through the formation of weak Fe(III) and Fe(II) complexes (19, 43). Nonetheless, it is clear that iron reduction is a part of iron solubilization (Fig. 2B) and likely contributes to the observed growth effects. These experiments show that under iron limitation, redox-active coumarins can enhance the growth yields of pseudomonads and that this can occur in fully oxic conditions.

Phenazines Can Enhance Iron-Limited Bacterial Growth under Hypoxic, Mildly Acidic Conditions. Phenazines are reduced by pseudomonads under a range of growth conditions (28, 29, 44), and under hypoxic and anoxic conditions, *Pseudomonas* cultures containing either endogenous or exogenous phenazines can reduce various iron sources (38, 44, 45). Hence, we suspected that in our experiments phenazines were also being reduced, but

that under oxic conditions, they failed to stimulate growth due to rapid oxidation by O₂ (21). To investigate this, we tested whether PCA promoted iron-limited growth under conditions of lower oxygen. Rather than switch to growth on anaerobic electron acceptors, which introduces complications (nitrate is the only anaerobic electron acceptor that promotes significant growth in *Pseudomonas* and N oxides generated during denitrification can react with iron and phenazines), we designed a set of experiments that allowed for a period of anoxia during which *Pseudomonas* would be able to reduce phenazines. These experiments mimic conditions that might occur in soils after rain events or within densely growing cultures (6, 46) and allow us to isolate the effects of oxygen without introducing fundamental changes in metabolism.

Cultures were grown under oxic conditions with 100 μM added PCA as previously described. However, in some treatments, flasks were allowed to stand statically for ~1 h (permitting oxygen depletion by respiration) before being returned to shaking (Fig. 4 A and B). Interestingly, when conducted at pH 7.5, this brief anoxic period was still insufficient to stimulate iron-limited growth. However, when conducted at pH 5.5, bacterial cultures allowed to sit statically for 1 h showed significantly ($P < 0.001$) increased cell densities over those that were shaken for the entire experiment (Fig. 4 A and B). Similar experiments at pH 5.5 with either fraxetin or no addition displayed little difference between “static” and shaking cultures. In experiments with *P. aeruginosa*, a few time points showed a slight elevation in OD in static treatments, possibly owing to reduction of endogenously produced phenazines.

Overall, these results confirm that the effect is due to PCA rather than to any artifacts associated with the treatment.

Measurements of dissolved oxygen during 1-h static incubation showed that oxygen is indeed drawn down to below detection limits at both pH 5.5 and pH 7.5 (Fig. 4C). Experiments at pH 7.5 exhibited slower oxygen consumption rates than at pH 5.5, likely due to slightly lower cell densities in these experiments (Fig. 4A). At high pH, iron is less available and hence final cell yields are lower (SI Appendix, Fig. S4 and Fig. 4 A and B) making it challenging to match cell densities between treatments. Nonetheless, in experiments at both pH 5.5 and pH 7.5 cells experienced ≥ 30 min of anoxia, hinting that differences in cellular PCA reduction rates, not just the rate of PCA oxidation by oxygen, may explain our results. We next sought to isolate the effect of pH on PCA reduction by conducting short-term assays of PCA reduction in the absence of oxygen. These experiments clearly showed higher PCA reduction rates at pH 5.5 vs pH 7.5 (Fig. 4D), consistent with previous work (47). The reason for this may be two-fold. First, PCA reduction is a proton coupled reaction (Fig. 2) and hence reduction is favored at low pH. In addition, PCA has a pKa of ~4.2 (48) and at high pH will occur as an anion, which may be less cell permeable, further decreasing cellular reduction rates. Together, these experiments demonstrate that both coumarins and phenazines can increase the growth yield of iron-limited pseudomonads but that these metabolites are useful in distinct chemical niches: with coumarins being largely beneficial under oxic and mildly alkaline conditions, and phenazines being most beneficial under hypoxic and acidic conditions.

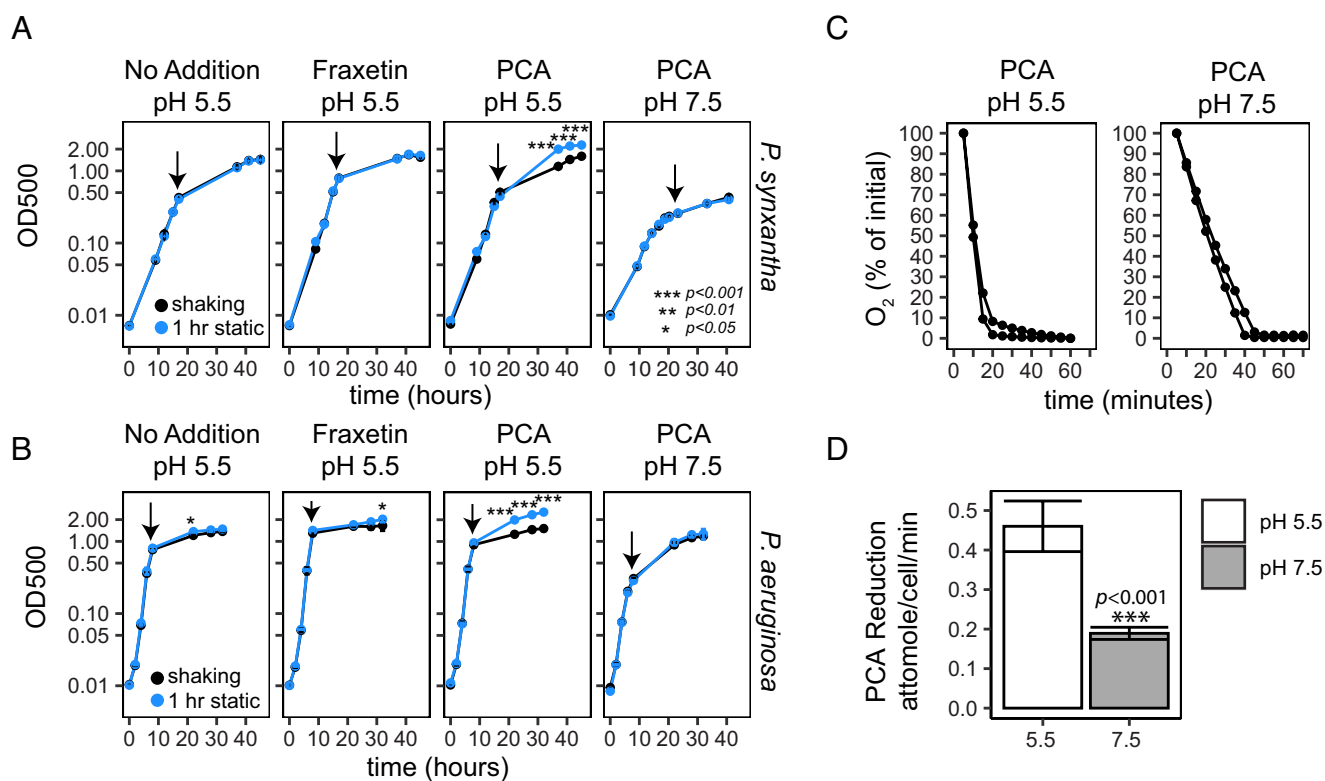


Fig. 4. PCA stimulates growth of pseudomonads under mildly acidic hypoxic conditions. (A and B) Growth of aerobic cultures of *P. synxantha* (A) and *P. aeruginosa* (B) maintained under continuous shaking (black) or allowed to sit statically for 1 h (blue, arrow indicates time point at which a 1 h static incubation was conducted) with: no addition, 100 μM PCA, or 100 μM fraxetin. Data shown are biological duplicates ±SD. (C) Oxygen consumption during *P. synxantha* 1 h static incubations with PCA (conducted at time point indicated by arrow in A) at pH 5.5 and 7.5. Each line represents one biological duplicate (growth data shown in A). (D) *P. synxantha* short-term PCA reduction rates at pH 5.5 and 7.5. To separate the effects of oxygen and pH, experiments were conducted in an anoxic chamber and reflect rates obtained over 60 min. Data shown are from quadruplicate incubations ±SD. All experiments (A–D) were conducted under iron limitation with HFO as the iron source and succinate as the carbon source. Significant differences between shaking and static treatments ((A and B), two-way ANOVA) are shown for each time point. Difference between PCA reduction rates were calculated using a two-way ANOVA comparing the effects of carbon source and pH (Materials and Methods and SI Appendix, Fig. S6).

The Use of Glucose as a Carbon Source Expands Bacterial Growth Promotion by Phenazines to Alkaline and Oxidic Conditions. Our experiments show distinct chemical microenvironments affect the utility of coumarin as opposed to phenazine metabolites with respect to iron acquisition. For phenazines, this occurs through an increase in phenazine reduction (at acidic pH) and/or a decrease in phenazine oxidation as driven by the depletion of oxygen by cellular respiration (Fig. 4C). Coumarins were less sensitive to changes in O_2 and pH, but did show the greatest increase in growth yields at alkaline pH (SI Appendix, Fig. S4). In these experiments, we used succinate as the carbon source, but glucose can also stimulate phenazine reduction (28, 29). Respiration may also be affected by carbon source, resulting in differential oxygen depletion. Given this, we wondered if different carbon sources supplied from plant roots might affect phenazine reduction.

To test this, we focused on comparisons between PCA and fraxetin, one of the coumarins showing the clearest bacterial growth stimulation under oxic conditions (Fig. 3 and SI Appendix, Fig. S4). We compared growth on exudate-relevant carbon sources with different oxidation states (C_{ox}): glucose ($C_{ox}:0$), succinate ($C_{ox}: +\frac{1}{2}$), and pyruvate ($C_{ox}: +\frac{2}{3}$) and performed a set of high-throughput plate reader experiments to test effects of pH and oxygen with these carbon sources. Duplicate microtiter plates were prepared containing treatments with either 100 μ M PCA, 100 μ M fraxetin, or no addition at pH 5.5 and 7.5 with each carbon source. Building on our findings showing a positive relationship between the rate of oxygen depletion and PCA growth

enhancement when shaken cultures were allowed to incubate statically (Fig. 4A–C), we used shaking and microbial respiration to tune oxygen availability. Plates were incubated in parallel, with one being shaken at high speeds to promote oxygenation and the other being shaken at slow speeds to allow for oxygen depletion. Consistent with our previous growth experiments (Fig. 3A and SI Appendix, Fig. S4), we found that when succinate was the carbon source fraxetin increased the final yield of iron-limited *P. synxantha* at both low and high pH and oxygen concentrations (fast shaking) but that PCA only stimulated growth at low pH and oxygen tensions (slow shaking), doing so more effectively than fraxetin under these conditions (Fig. 5). We observed similar trends when equimolar amounts of C in the form of pyruvate were used as the carbon source. In contrast, when equimolar concentrations of C as glucose were used, PCA increased yields even at fast shaking speeds and high pH (Fig. 5).

The apparent promotion of phenazine reduction by glucose, the most reduced of our carbon substrates, is consistent with previous findings (28, 29). However, in our experiments, it remains unclear whether this is a direct effect of changes in PCA reduction rate, possibly due to increased reducing power, or an additive (or sole) effect of changes in respiration rates drawing down oxygen and thus alleviating PCA oxidation. Our short-term PCA reduction rate experiments show clear differences between pH 5.5 and pH 7.5 (SI Appendix, Fig. S6B) for all carbon sources relative to themselves (Fig. 4D and SI Appendix, Fig. S6). At pH 5.5, we observed significantly ($P < 0.001$) greater PCA reduction rates

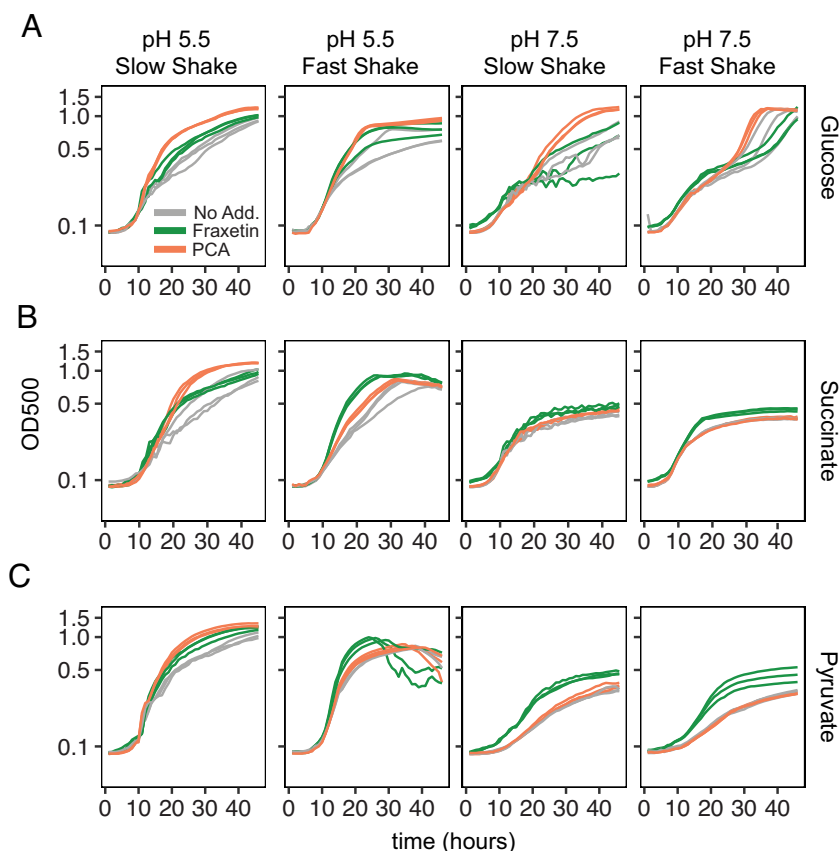


Fig. 5. Carbon source tunes the effects of PCA on *P. synxantha*. Growth of *P. synxantha* with HFO as the iron source and glucose (A), succinate (B), or pyruvate (C) as the carbon source. Metabolites were added at a final concentration of 100 μ M and experiments were conducted under ambient oxygen conditions. Slow shaking speeds allow microbial respiration to decrease oxygen, while faster speeds maintain higher oxygen tensions. When succinate and pyruvate are the carbon source PCA primarily stimulates growth yields at slow shaking speeds and at pH 5.5. However, growth on glucose allows PCA to enhance growth yields at high shaking speeds and pH 7.5. Three biological replicates are shown as individual lines. Statistical significance is shown in SI Appendix, Fig. S7. See also SI Appendix, Fig. S8 for replicate experiments showing consistency in broad trends. Total carbon was kept constant across treatments.

when cells were supplied with glucose vs succinate or pyruvate (*SI Appendix, Fig. S6*). However, there was no difference in reduction rates on different sugars at pH 7.5 and in some cases reduction rates appeared higher on pyruvate than on the other sugars, an observation that has been made in other experimental contexts (29). Direct measurements of oxygen in our experiments are not possible given current technologies (49) as any disturbance in shaking would alter oxygen tensions precluding an accurate measurement of the oxygen concentrations experienced by cells. Succinate and pyruvate are both organic acids, and despite medium buffering (which cannot be increased due to toxicity concerns), it is also possible that shifts toward more alkaline pH during growth on these substrates further decrease PCA reduction (50). However, pH changes are unlikely to explain differences in PCA reduction between succinate and glucose seen in short-term experiments (*SI Appendix, Fig. S6*). Whether one or multiple mechanisms are at work, our experiments show that the carbon source can have important effects on secondary metabolite function. This finding suggests that changes in carbon exudation by plant roots may tune the utility of secondary metabolites produced by their microbiome.

Implications for RAM Chemical Ecology in the Rhizosphere. An important next step in for studying RAM chemical ecology in the rhizosphere will be understanding the spatial and temporal dynamics of RAM production, the quantities in which RAMs are produced, and the physicochemical properties of the microenvironments in which they are found. Coumarin secretion is spatially discrete in plant roots, with different coumarins being released from different parts of the root (51, 52), possibly creating microzones with very high concentrations of specific coumarins. For instance, despite the limited iron-solubilizing capacity of scopoletin (Fig. 2*B*), many previous studies have reported high concentrations of this coumarin in iron-limited *A. thaliana* roots exudates (4, 17). Sideritin, a more newly characterized coumarin (which was not tested here as synthetic standards are not available), also appears to be both highly efficient at iron reduction and abundant in *A. thaliana* root exudates (19). Interestingly, abiotic reactions between Fe(III) and scopoletin can lead to the generation of more effective iron-solubilizing coumarins including sideretin and fraxetin (37, 43), raising the possibility that scopoletin secretion (especially at high concentrations) might be more useful for iron solubilization in situ than it appears based on our in vitro studies.

Indeed, we still have much to learn regarding the ways RAMs interact with other iron-solubilizing molecules. The evidence from abiotic experiments indicates that RAMs and siderophores can act synergistically to solubilize iron (53, 54). The exact chemical mechanisms are not clear but one suggestion has been that siderophores might bind and stabilize iron that is solubilized by RAMs (53). Our experiments with siderophore-null *P. aeruginosa* strains still showed enhanced growth yields in the presence of coumarins (*SI Appendix, Fig. S5*) demonstrating that pseudomonads can benefit from coumarin-solubilized iron in the absence of siderophores. Whether this occurs through direct uptake of Fe(II), uptake of coumarin–Fe(II)/Fe(III) chelates, or another mechanism will also be an important area for future investigation.

The genetic regulation of RAM biosynthesis and the related question of whether plants and microbes experience iron limitation at similar or different environmental concentrations could also carve out different niches for rhizosphere secondary metabolites. The controls on plant coumarin secretion are complex, integrating above and belowground signals (52). In addition to potential abiotic interactions with siderophores, RAMs may also

alter the biosynthesis of these iron-solubilizing metabolites. For instance, siderophores are strongly regulated by iron in most bacteria and several studies have shown that iron privatization by siderophores shifts the composition of synthetic rhizosphere communities (2, 15). An excess supply of iron provided by RAMs could decrease siderophore production, allowing different groups of microbes, be they plant friends or foes, to proliferate.

While our study emphasizes the growth benefits of coumarins, previous work has shown that coumarins can be toxic to rhizosphere microbes, including pseudomonads (3, 4). This toxicity has been attributed to the generation of ROS (3), likely through the reduction of Fe(III) to Fe(II) and subsequent Fenton reactions (26, 27, 55, 56). Our results suggest that coumarin toxicity may depend on the environmental context as well as the organisms being studied. In some cases, coumarin toxicity towards pseudomonads has been reported under iron-replete conditions (57, 58). When there is little benefit to be had from coumarins, it stands to reason that ROS toxicity may dominate the growth response, as seen in our experiments under nitrogen limitation (Fig. 3). However, plant–microbe coculturing experiments have also shown that under iron limitation, coumarin biosynthesis by the plant selects against a specific pseudomonad (3). These experiments used a synthetic microbial community and allowed for endogenous coumarin production by *A. thaliana* and therefore may capture dynamics absent in our experimental system. It is also possible that these contrasting results are explained by differences in ROS sensitivities between pseudomonad species. For example, previous work has shown elevated coumarin tolerance in certain pseudomonads (4). Understanding the physiological underpinnings of these different coumarin effects is of interest both within the rhizosphere and beyond as coumarins have been the topic of intense pharmaceutical interest and have been investigated as potential antimicrobials for opportunistic human pathogens, including *P. aeruginosa* (57–59).

Conclusion

Our work demonstrates that chemically distinct redox-active soil secondary metabolites function differently under varying oxygen, pH, and carbon regimes with respect to iron acquisition. A straightforward expectation from our work is that in more alkaline and well-drained (and hence oxic) soils coumarins may be more important for RAM-based iron solubilization than phenazines. More generally, our findings provide a proof-of-principle demonstration that the paradox of secondary metabolite redundancy may be resolved, in part, by considering their chemical ecological niche at high spatiotemporal resolution. However, we do not fully understand the extent to which the chemical parameters found in bulk soil and parent material are maintained in the microenvironment experienced at the plant root. Indeed, our findings indicate that couplings between plant and microbial metabolisms—through carbon release by plants and oxygen consumption by microbes—can profoundly affect the chemical microenvironment and the biological impact of secondary metabolites. A grand future challenge is determining how in situ rhizosphere conditions change over space and time.

Materials and Methods

Electrochemical Measurements. Cyclic voltammetry (CV) measurements were conducted using a BioLogic SP-300 potentiostat with a scan rate of 50 mV/s using a platinum wire counter electrode and an Ag/AgCl reference. A 3-mm gold working electrode (BASi) was used for experiments with coumarins. We initially conducted PCA CV using a gold electrode; however, we observed deviations from Nernstian

conditions at pH 7.5, as has been previously noted and attributed to potential adsorption at the electrode surface (21). Hence, PCA experiments were repeated with a 3 mm glassy carbon electrode (BASi) which produced better results. 10 mM solutions of coumarins (coumarin, daphnetin, fraxetin, and scopoletin) were prepared in ethanol and stored at -20°C . Before measurements, solutions were diluted tenfold to 1 mM in 1M potassium chloride (KCl) buffered with 10 mM ammonium acetate-MOPS, at pH 5.5, 6.5, or 7.5. PCA (10 mM) was prepared in 20 mM MES buffer, stored at 4°C , and diluted to 1 mM (as above). Coumarin CV experiments were conducted under ambient oxygen conditions (benchtop). For PCA, solutions were purged with N_2 , and measurements were conducted under a continuous N_2 stream. Data shown are generally the second of three scans; however for scopoletin, the first scan is shown due to obvious irreversible redox reactions (as previously documented (37), see *SI Appendix, Fig. S1* for full scans).

Ferrozine Assays for Fe(III) Reduction. Abiotic ferrozine assays (60) were conducted in 100 mM MES buffered at pH 5.5 or 100 mM MOPS buffered at pH 7.5 using a final concentration of $40\ \mu\text{M}$ FeCl_3 (maintained as a concentrated stock in 0.1N HCl), $20\ \mu\text{M}$ metabolite, and 2 mM ferrozine. The precipitation of hydrous ferric oxide may occur within the timescales of our experiments, and hence, ferrozine assays may reflect reduction of Fe(III) at the mineral surface rather than in solution. Anoxic experiments were assembled inside an anoxic chamber (Coy) under a 95% N_2 , 5% H_2 atmosphere and conducted using a plate reader (BioTek, Synergy HTX) housed within the chamber. Ferrozine, MES, and FeCl_3 solutions were passively degassed inside the chamber for 3 d before the start of experiments. Metabolites were not degassed but were added at 1% of the total volume. The ferrozine-Fe(II) complex was detected via absorbance at 562 nm and concentrations were determined using an Fe(II) standard curve. Oxidic experiments were assembled at the benchtop and conducted using a benchtop plate reader (BioTek, Epoch 2). Coumarin and oxidized PCA stocks were maintained as described above. Reduced PCA was prepared through electrochemical reduction and stored in a stoppered bottle under a pure N_2 headspace. Small aliquots were withdrawn (in the chamber) immediately before the start of experiments. For oxidic experiments, a small aliquot of reduced PCA was removed from the anoxic chamber and added to experimental wells immediately before the start of experiments, to capture the oxidation of the metabolite. For control experiments using Fe(II), solutions of FeCl_2 were prepared in an anaerobic chamber using deoxygenated water. These solutions were then either added to 96-well plates containing deoxygenated ferrozine-MES/MOPS solutions or removed from the anaerobic chamber and added to fully oxygenated ferrozine-MES/MOPS solutions under ambient air. In both cases, the formation of the Fe(II)-ferrozine complex was detected at 562 nm.

Strains and Experimental Growth Conditions. *Pseudomonas aeruginosa* PA14 and *Pseudomonas synxantha* 2-79 (formerly *P. fluorescens*) were maintained as freezer stocks. Mutant *P. aeruginosa* strains in which key biosynthetic genes for the siderophores pyoverdine and pyochelin have been deleted ($\Delta pvdA\Delta pchE$, herein ΔSid) were generated previously (25). Before the start of each experiment strains were struck onto LB-agar plates. Cells were then pregrown in a defined growth medium containing: 4.1×10^{-4} M $\text{MgSO}_4 \cdot 7\text{H}_2\text{O}$, 6.8×10^{-4} M $\text{CaCl}_2 \cdot 2\text{H}_2\text{O}$, 1.6×10^{-2} M NH_4Cl , 4.7×10^{-3} M KH_2PO_4 , 2.3×10^{-3} M K_2HPO_4 and 3.7×10^{-2} M succinate as the carbon source. The growth medium was buffered at pH 7.5 with 20 mM MOPS and prepared in acid cleaned polycarbonate or polystyrene bottles. With the exception of growth medium for initial PA14 Fe-limitation experiments (Fig. 3B and *SI Appendix, Fig. S5*), all media was passed through a chelex column [prepared according to (61)] in order to strip background iron. After chelating, the medium pH was checked and adjusted as needed using NaOH or HCl, and media were then supplemented with Aquil trace metals (61) without added iron or ethylenediaminetetraacetic acid (EDTA) and filter sterilized (Stericup, $0.22\ \mu\text{m}$ polyethersulfone membrane, Millipore-Sigma). Inductively coupled plasma mass spectrometry (ICP) measurements showed background iron concentrations of ~ 50 to $100\ \text{nM}$ in cleaned media. A minimum of two transfers (1:100 dilution, at ~ 24 h intervals) in this no-iron medium were conducted before the start of each experiment. Large volume flask experiments were conducted using 20 mL of culture in 25-cm^2 tissue culture flasks with vented caps (Falcon, cat# 35-3108) at 30°C (*P. synxantha*) or 37°C (*P. aeruginosa*) with constant shaking at 250 rpm. To promote aeration, flasks were oriented with their longest side secured to the incubator plate, thus maximizing the air-liquid interface. Nitrogen limited experiments were conducted as above, with the following exceptions: acid-cleaning

and chelex steps were omitted, HFO was substituted with $100\ \mu\text{M}$ EDTA and $10\ \mu\text{M}$ Fe, and nitrogen concentrations were lowered to 2×10^{-3} M NH_4Cl .

To initiate experiments, cells were centrifuged at $6,800 \times g$ for 10 min and resuspended in growth medium without additions. Washed cells were then added to each treatment at a final OD of 0.01. Typical additions were $500\ \mu\text{L}$ cells to 20 mL media. HFO was prepared using the recipe for two-line ferrihydrite (62) see also ref. 45 and stored at -80°C . Before the start of experiments, 8.4 mg of HFO was resuspended in 10 mL of MQ water, this slurry was then diluted 1:100 into experimental treatments. Coumarins and PCA were maintained in 10 mM stocks as described above and added at final concentrations of $100\ \mu\text{M}$ for all experiments. A 1% final concentration of ethanol was added to control and +PCA treatments in order to match the concentration introduced with coumarin additions. In order to minimize artifacts from differences in abiotic reaction times, HFO and metabolite media mixtures were prepared immediately before the start of experiments. HFO was always added before metabolites and cells were added as quickly as possible thereafter. An effort was also made to minimize exposure to light during medium preparation and experimental incubations. Culture growth was determined using optical density (OD) measurements at 500 nm (DU-800 spectrophotometer, Beckman-Coulter), and flasks were removed from the incubator in small batches to minimize the amount of time that cultures were allowed to sit static during subsampling for OD measurements. For plate reader experiments with all added coumarins (*SI Appendix, Fig. S4*) the techniques described above were used; however, 20 mM MES buffer was used for pH 5.5 and pH 6.5 experiments. In addition, cells were precultured at pH 6.5 and then diluted into pH 5.5, 6.5 or 7.5 experimental media.

Shaking-Static Incubation Experiments and Oxygen Measurements. Medium preparation, pregrowth, and growth conditions were performed as described above. At the indicated time static treatment flasks were removed from the shaking incubator, placed upright and allowed to sit without shaking for 1 h. *P. aeruginosa* static incubations were heated to 37°C . *P. synxantha* static incubations were performed at room temperature (to accommodate the instrumentation for the oxygen probes in + PCA treatments, all treatments were kept at room temperature for consistency). Oxygen measurements were made by directly inserting probes into the culture. All experiments used amperometric Clark-type electrodes. Experiments at pH 5.5 used Oxyferm FDA sensors (Hamilton), whereas those at pH 7.5 used Unisense oxygen microsensors, for these experiments, cultures were transferred to 50 mL conical tubes during incubations to accommodate differently sized probes. Oxyferm probes were calibrated immediately before the start of experiments using air and N_2 sparged water as the 100% and 0% O_2 , respectively. Unisense probes were calibrated using growth medium and a $-0.1\ \text{M}$ NaOH/ $0.1\ \text{M}$ ascorbate solution as 100% and 0% O_2 , respectively. Oxygen data are reported relative to initial conditions and therefore should not be affected by any differences between probes.

Slow- and Fast-Shaking Plate Reader Experiments. For plate reader experiments, growth medium was prepared as described above. However, MES buffer (20 mM) was used for pH 5.5 and pH 6.5 experiments. Equimolar concentrations of carbon (148 mM C) were maintained across succinate, glucose and pyruvate experiments. Experiments were performed in clear 96-well plates using $200\ \mu\text{L}$ final volume. Cells were pre-grown with the indicated carbon source at pH 6.5 and were washed and resuspended in pH 6.5 medium with either succinate, glucose or pyruvate before being inoculated into different pH conditions. Cells were added at a final OD of ~ 0.01 , typically as a 5 to $10\ \mu\text{L}$ addition. Experiments were conducted using a BioTek Epoch 2 Plate Reader on the bench top. Orbital shaking was set at either 807 cpm and 1 mm orbital diameter (fast shaking) or 187 cpm and 6 mm orbital diameter (slow shaking), and plates were incubated with lids on. Slow- and fast-shaking plates were set up in parallel using the same inoculum (for each carbon source) and experiments were run simultaneously in two side-by-side plate readers.

Short-Term PCA Reduction Rates. Cells were pre-grown as described above with a minimum of two transfers before the start of experiments. For Fe-limited experiments (Fig. 4D and *SI Appendix, Fig. S6A*), cells were acclimated at pH 6.5 in a medium without iron with the indicated carbon source. To initiate Fe-limited experiments, cells were grown (aerobically) to an OD of 0.5 to 0.7 in a medium containing HFO (prepared as above), $100\ \mu\text{M}$ PCA and the indicated carbon source before being centrifuged at $6,800 \times g$ for 10 min and resuspended in

pH 6.5 media without iron or PCA. A small inoculum of this cell slurry was then added at a final OD of ~0.2 to degassed media buffered at pH 5.5 or 7.5 with the appropriate carbon source and without added iron. Cells were incubated in an anoxic chamber (95% N₂, 5% H₂ atmosphere) for 1 h to allow full oxygen depletion and then spiked with 100 μM oxidized PCA. PCA reduction rates were measured via fluorescence [excitation at 360 nm, emission at 528 nm, (63)] on a plate reader (Synergy HTX, BioTek) housed within an anoxic chamber. The fluorescence of the siderophore pyoverdine (max excitation/emission typically 360 to 410 nm and 450 to 480 nm, respectively) interferes with measurements of PCA reduction—we initially attempted to measure PCA reduction directly during anoxic incubations (Fig. 4 A and B) but were unsuccessful due to interference from high concentrations of pyoverdine in the medium. The washing procedure described herein successfully allowed for the detection of changes in PCA reduction over time, however we still observed relatively high initial fluorescence, possibly due to cell-associated pyoverdines being not removed during washing. As such, we conducted later reduction assays under Fe-replete conditions where siderophore production is not expected (SI Appendix, Fig. S6B). For these experiments, the procedures used were as described above with the exception that all steps used a medium with 100 μM EDTA and 10 μM Fe. Fe-limited and Fe-replete reduction rates were largely in agreement (compare SI Appendix, Fig. S6 A and B). All rates were calculated from 1 h of data collected between 30 and 90 min after the start of experiments. PCA concentrations were determined by comparison to a standard curve of electrochemically reduced PCA. Per cell reduction rates were calculated assuming 10⁹ cell mL⁻¹ OD⁻¹.

Statistical Analysis. All statistical analysis was performed in R (64) using ANOVA and Tukey's post hoc test. For differences in large volume growth yields (Fig. 3),

a one-way ANOVA was conducted on data from the final time point in all experiments. Only statistical differences between untreated controls and treatments are reported. Significant differences between shaking and static treatments (Fig. 4 A and B) were conducted using a two-way ANOVA (testing for treatment*time) across all time points. Significant differences in PCA reduction rates (reported in Fig. 4D and SI Appendix, Fig. S6) were determined using one and two-way ANOVA: For Fe-limited experiments, pH 5.5 and 7.5 data were combined and the effect of rate by pH and sugar was tested and reported (two-way ANOVA). For Fe-replete experiments, a one-way ANOVA was conducted on rate by sugar for pH 5.5 data only (due to lack of detectable rates at pH 7.5). For fast- and slow-shaking experiments (SI Appendix, Figs. S7 and S8) a one-way ANOVA was conducted at the indicated time points.

Data, Materials, and Software Availability. All study data are included in the article and/or SI Appendix.

ACKNOWLEDGMENTS. We thank S. Wilbert for help with dissolved oxygen measurements. This work was supported by a grant from the NIH (1R01AI127850-01A1) to D.K.N. D.L.M. was supported by a division postdoctoral fellowship from Biology and Biological Engineering at Caltech, the Simons Foundation Marine Microbial Ecology postdoctoral fellowship and the L'Oréal USA for Women in Science postdoctoral fellowship.

Author affiliations: ^aDivision of Biology and Biological Engineering, California Institute of Technology, Pasadena, CA 91125; and ^bDivision of Geological and Planetary Sciences, California Institute of Technology, Pasadena, CA 91125

- S. L. Lebeis *et al.*, Salicylic acid modulates colonization of the root microbiome by specific bacterial taxa. *Science* **349**, 860–864 (2015).
- S. Gu *et al.*, Competition for iron drives phytopathogen control by natural rhizosphere microbiomes. *Nat. Microbiol.* **484**, 186–189 (2020).
- M. J. E. E. Voges, Y. Bai, P. Schulze-Lefert, E. S. Sattely, Plant-derived coumarins shape the composition of an *Arabidopsis* synthetic root microbiome. *Proc. Natl. Acad. Sci. U.S.A.* **116**, 12558–12565 (2019).
- I. A. Stringlis *et al.*, MYB72-dependent coumarin exudation shapes root microbiome assembly to promote plant health. *Proc. Natl. Acad. Sci. U.S.A.* **115**, E5213–E5222 (2018).
- E. G. Wilbanks *et al.*, Microscale sulfur cycling in the phototrophic pink berry consortia of the Sippewissett salt marsh. *Environ. Microbiol.* **16**, 3398–3415 (2014).
- M. Keilueit *et al.*, Mineral protection of soil carbon counteracted by root exudates. *Nat. Clim. Change* **5**, 588–595 (2015).
- E. S. Cowley, S. H. Kopf, A. LaRiviere, W. Ziebis, D. K. Newman, Pediatric cystic fibrosis sputum can be chemically dynamic, anoxic, and extremely reduced due to hydrogen sulfide formation. *mBio* **6**, e00767 (2015).
- B. Borer, R. Tecon, D. Or, Spatial organization of bacterial populations in response to oxygen and carbon counter-gradients in pore networks. *Nat. Commun.* **9**, 1–11 (2018).
- C. M. Palmer, M. L. Gueriot, Facing the challenges of Cu, Fe and Zn homeostasis in plants. *Nat. Chem. Biol.* **5**, 333–340 (2009).
- R. C. Hider, X. Kong, Chemistry and biology of siderophores. *Nat. Prod. Rep.* **27**, 637–657 (2010).
- O. X. Cordero, L.-A. Ventouras, E. F. DeLong, M. F. Polz, Public good dynamics drive evolution of iron acquisition strategies in natural bacterioplankton populations. *Proc. Natl. Acad. Sci. U.S.A.* **109**, 20059–20064 (2012).
- A. D'Onofrio *et al.*, Siderophores from neighboring organisms promote the growth of uncultured bacteria. *Chem. Biol.* **17**, 254–264 (2010).
- M. F. Traxler, M. R. Seyedsayamdost, J. Clardy, R. Kolter, Interspecies modulation of bacterial development through iron competition and siderophore piracy. *Mol. Microbiol.* **86**, 628–644 (2012).
- J. Granger, N. M. Price, The importance of siderophores in iron nutrition of heterotrophic marine bacteria. *Limnol. Oceanogr.* **44**, 541–555 (1999).
- L. Xu *et al.*, Genome-resolved metagenomics reveals role of iron metabolism in drought-induced rhizosphere microbiome dynamics. *Nat. Commun.* **12**, 1–17 (2021).
- I. A. Stringlis, R. De Jonge, C. M. J. Pieterse, The age of coumarins in plant-microbe interactions. *Plant Cell Physiol.* **60**, 1405–1419 (2019).
- P. Fourcroy *et al.*, Involvement of the ABCG37 transporter in secretion of scopoletin and derivatives by *Arabidopsis* roots in response to iron deficiency. *New Phytol.* **201**, 155–167 (2014).
- N. B. Schmid, R. Giehl, S. Döll, H. M. Plant, 2014, Feruloyl-CoA 6'-Hydroxylase1-dependent coumarins mediate iron acquisition from alkaline substrates in *Arabidopsis*. *Plant Physiol.* **164**, 160–172 (2014).
- J. Rajniak *et al.*, Biosynthesis of redox-active metabolites in response to iron deficiency in plants. *Nat. Chem. Biol.* **14**, 442–450 (2018).
- C. J. Harbort *et al.*, Root-secreted coumarins and the microbiota interact to improve iron nutrition in *Arabidopsis*. *Cell Host Microbe* **28**, 1–20 (2020).
- Y. Wang, D. K. Newman, Redox reactions of phenazine antibiotics with ferric (hydr)oxides and molecular oxygen. *Environ. Sci. Technol.* **42**, 2380–2386 (2008).
- S. Chincholkar, L. S. Thomashow, *Microbial Phenazines* (Springer, Berlin, Heidelberg, 2013).
- A. Price-Whelan, L. E. P. Dietrich, D. K. Newman, Rethinking 'secondary metabolism': Physiological roles for phenazine antibiotics. *Nat. Chem. Biol.* **2**, 71–78 (2006).
- D. Dar, L. S. Thomashow, D. M. Weller, D. K. Newman, Global landscape of phenazine biosynthesis and biodegradation reveals species-specific colonization patterns in agricultural soils and crop microbiomes. *eLife* **9**, 223 (2020).
- Y. Wang *et al.*, Phenazine-1-carboxylic acid promotes bacterial biofilm development via ferrous iron acquisition. *J. Bacteriol.* **193**, 3606–3617 (2011).
- P. Ashworth, Electron spin resonance studies of structure and conformation in anion radicals formed during the autoxidation of hydroxylated coumarins. *J. Org. Chem.* **41**, 2920–2924 (1976).
- C. E. Ofoedu *et al.*, Hydrogen peroxide effects on natural-sourced polysaccharides: Free radical formation/production, degradation process, and reaction mechanism—a critical synopsis. *Foods* **10**, 699 (2021).
- Y. Wang, S. E. Kern, D. K. Newman, Endogenous phenazine antibiotics promote anaerobic survival of *Pseudomonas aeruginosa* via extracellular electron transfer. *J. Bacteriol.* **192**, 365–369 (2010).
- N. R. Glasser, B. X. Wang, J. A. Hoy, D. K. Newman, The pyruvate and α-ketoglutarate dehydrogenase complexes of *Pseudomonas aeruginosa* catalyze pyocyanin and phenazine-1-carboxylic acid reduction via the subunit dihydrolipoamide dehydrogenase. *J. Biol. Chem.* **292**, 5593–5607 (2017).
- P. B. Larsen *et al.*, Aluminum-resistant *Arabidopsis* mutants that exhibit altered patterns of aluminum accumulation and organic acid release from roots. *Plant Physiol.* **117**, 9–18 (1998).
- K. Zhalina *et al.*, Dynamic root exudate chemistry and microbial substrate preferences drive patterns in rhizosphere microbial community assembly. *Nat. Microbiol.* **3**, 470–480 (2018).
- J. M. Chaparro *et al.*, Root exudation of phytochemicals in *Arabidopsis* follows specific patterns that are developmentally programmed and correlate with soil microbial functions. *PLoS One* **8**, e55731 (2013).
- P. Mladěnka *et al.*, In vitro interactions of coumarins with iron. *Biochimie* **92**, 1108–1114 (2010).
- N. Elgrishi *et al.*, A practical beginner's guide to cyclic voltammetry. *J. Chem. Educ.* **95**, 197–206 (2017).
- A. Vogel, Darstellung von benzoessäure aus der tonka-bohne und aus den meliloten - oder steinklee - blumen. *Annalen der Physik* **64**, 161–166 (1820).
- D. Mavrodi *et al.*, Accumulation of the antibiotic phenazine-1-carboxylic acid in the rhizosphere of dryland cereals. *Appl. Environ. Microbiol.* **78**, 804–812 (2012).
- K. C. d. S. Leite, *et al.*, Electrochemical characterization of scopoletin, a 7-hydroxy-6-methoxy-coumarin. *Int. J. Electrochem. Sci.* **10**, 5714–5725 (2015).
- C. D. Cox, Role of pyocyanin in the acquisition of iron from transferrin. *Infect. Immun.* **52**, 263–270 (1986).
- W. Stumm, G. F. Lee, Oxygenation of ferrous iron. *ACS Publ.* **53**, 143–146 (1961).
- D. Mavrodi, W. Blankenfeldt, L. S. Thomashow, Phenazine compounds in fluorescent *Pseudomonas* spp. biosynthesis and regulation. *Annu. Rev. Phytopathol.* **44**, 417–445 (2006).
- C. D. Cox, Iron uptake with ferripyochelin and ferric citrate by *Pseudomonas aeruginosa*. *J. Bacteriol.* **142**, 581–587 (1980).
- C. D. Cox, P. Adams, Siderophore activity of pyoverdine for *Pseudomonas aeruginosa*. *Infect. Immun.* **48**, 130–138 (1985).
- M. Baune *et al.*, Importance of oxidation products in coumarin-mediated Fe(hydr)oxide mineral dissolution. *BioMetals* **33**, 305–321 (2020).
- M. E. Hernandez, A. Kappler, D. K. Newman, Phenazines and other redox-active antibiotics promote microbial mineral reduction. *Appl. Environ. Microbiol.* **70**, 921–928 (2004).
- D. L. McRose, D. K. Newman, Redox-active antibiotics enhance phosphorus bioavailability. *Science* **371**, 1033–1037 (2021).
- C. M. VanDrise, R. Lipsh-Sokolik, O. Khersonsky, S. J. Fleishman, D. K. Newman, Computationally designed pyocyanin demethylase acts synergistically with tobramycin to kill recalcitrant *Pseudomonas aeruginosa* biofilms. *Proc. Natl. Acad. Sci. U.S.A.* **118**, e2022012118 (2021).

47. E. K. Perry, D. K. Newman, Prevalence and correlates of phenazine resistance in culturable bacteria from a dryland wheat field. *Appl. Environ. Microbiol.* **88**, e02320 (2022).
48. P. G. Brisbane, L. J. Janik, M. E. Tate, R. F. Warren, Revised structure for the phenazine antibiotic from *Pseudomonas fluorescens* 2-79 (NRRL B-15132). *Antimicrob. Agents Chemother.* **31**, 1967-1971 (1987).
49. A. I. Flamholz, S. Saccomano, K. Cash, D. K. Newman, Optical O₂ sensors also respond to redox active molecules commonly secreted by bacteria. *mBio* **13**, e0207622 (2022).
50. R. Sánchez-Clemente, Study of pH changes in media during bacterial growth of several environmental strains. *Proceedings* **2**, 1297 (2018).
51. K. Robe *et al.*, Coumarin accumulation and trafficking in *Arabidopsis thaliana*: A complex and dynamic process. *New Phytol.* **229**, 2062-2079 (2021).
52. C. Zamioudis *et al.*, Rhizobacterial volatiles and photosynthesis-related signals coordinate MYB72 expression in *Arabidopsis* roots during onset of induced systemic resistance and iron-deficiency responses. *Plant J.* **84**, 309-322 (2015).
53. Z. Wang, W. D. C. Schenkeveld, S. M. Kraemer, D. E. Giammar, Synergistic effect of reductive and ligand-promoted dissolution of goethite. *Environ. Sci. Technol.* **49**, 7236-7244 (2015).
54. W. D. C. Schenkeveld, Z. Wang, D. E. Giammar, S. M. Kraemer, Synergistic effects between biogenic ligands and a reductant in Fe acquisition from calcareous soil. *Environ. Sci. Technol.* **50**, 6381-6388 (2016).
55. M. E. Medina, C. Iuga, J. R. Álvarez-Idaboy, Antioxidant activity of fraxetin and its regeneration in aqueous media. A density functional theory study. *RSC. Adv.* **4**, 52920-52932 (2014).
56. H. Boulebd, I. A. Khodja, A detailed DFT-based study of the free radical scavenging activity and mechanism of daphnetin in physiological environments. *Phytochemistry* **189**, 112831 (2021).
57. R. E. D'almeida *et al.*, Comparison of seven structurally related coumarins on the inhibition of quorum sensing of *Pseudomonas aeruginosa* and *Chromobacterium violaceum*. *Bioorg. Chem.* **73**, 37-42 (2017).
58. Z. Ye *et al.*, Effects of daphnetin on biofilm formation and motility of *Pseudomonas aeruginosa*. *Front. Cell. Infect. Microbiol.* **12**, 1033540 (2022).
59. F. Borges, F. Roleira, N. Milhazes, L. Santana, E. Uriarte, Simple coumarins and analogues in medicinal chemistry: Occurrence, synthesis and biological activity. *Curr. Med. Chem.* **12**, 887-916 (2005).
60. L. L. Stookey, Ferrozine—a new spectrophotometric reagent for iron. *Anal. Chem.* **42**, 779-781 (1970).
61. N. M. Price *et al.*, Preparation and chemistry of the artificial algal culture medium aquil. *Biol. Oceanogr.* **6**, 443-461 (1989).
62. U. Schwertmann, R. Cornell, *Iron Oxides in the Laboratory: Preparation and Characterization* (Wiley, 2000).
63. N. L. Sullivan, D. S. Tzeranis, Y. Wang, P. T. C. So, D. K. Newman, Quantifying the dynamics of bacterial secondary metabolites by spectral multiphoton microscopy. *ACS Chemical Biol.* **6**, 893-899 (2011).
64. RCoreTeam, R: A language and environment for statistical computing (R Studio 2022.07.2, R Foundation for Statistical Computing) (2021).